Axel: A Minimalist Tethered Rover for Exploration of Extreme Planetary Terrains

Pablo Abad-Manterola, Jeff Edlund, Joel Burdick, Albert Wu, Thomas Oliver
California Institute of Technology
Pasadena, CA 91125

Issa A.D. Nesnas
Jet Propulsion Laboratory
California Institute of Technology
Pasadena, CA 91109

Johanna Cecava
Marshall Space Flight Center
Huntsville, AL 35812

Abstract—Recent scientific findings suggest that some of the most interesting sites for future exploration of planetary surfaces lie in terrains that are currently inaccessible to conventional robotic rovers. In order to provide robust and flexible access to these terrains we have been developing the "Axel" robotic rover. Axel is a lightweight 2-wheeled vehicle that can access steep terrains and negotiate relatively large obstacles due to its actively managed tether and novel wheel design. This paper reviews the Axel system and focuses on those system components that affect Axel's steep terrain mobility. Experimental demonstrations of Axel on sloped and rocky terrains are presented.

1. MOTIVATION

Despite the great successes of the Mars Exploration Rovers [1], some of the richest potential science targets for future exploration missions lie in terrains that are inaccessible to state-of-the-art Martian rovers, thereby limiting our ability to carry out *in situ* analysis of these rich opportunities. For example, bright new deposits, which may be ice flows, have been discovered hundreds of meters below the rims of steep craters in the Centauri Montes regions on Mars (Figure 1). While the Opportunity rover has imaged layers of bedrock in the vertical promontories of Cape St. Vincent in Victoria crater, these geological features are currently inaccessible to conventional sampling methods. High-resolution orbiter images of stratified deposits of ice and dust reveal a very challenging terrain, which if it could be navigated, would provide important clues to the geological and hydrological past of Mars [2]. The recently reported Martian methane plumes [3] rise over heavily cratered terrains in the Arabia Terra and Syrtis Major regions. Without new mobility platforms, it will be difficult to directly access the surface of this region to assess if the methane comes from a biological or geological origin. Similarly, Titan, Europa, Enceladus, and the Earth's moon also offer challenging surface features with associated scientific targets. A new generation of planetary exploration robots is needed to access the challenging terrains in order to probe, sample and measure. New inquiries of this sort could lead to significant scientific rewards.

2. ROBOTIC MOBILITY FOR EXTREME TERRAIN

Mechanisms and algorithms for robotic mobility in steep and complex terrains have been investigated for several decades. Proposed approaches include multi-legged quasi-static walkers [4], bipedal walkers [5], hopping machines [6], snake-like mechanisms [7], and wheeled vehicles with complex wheel designs [8] or chassis [9]. Critical issues in evaluating the viability of these approaches for space applications include the robustness and mechanical complexity inherent with the approach, the total system mass, the energy required per traverse distance, the ability to carry out *in situ* scientific studies and sample gathering, and the ability to recover from faults. Most previously proposed methods have one or more shortcomings with respect to these criteria.

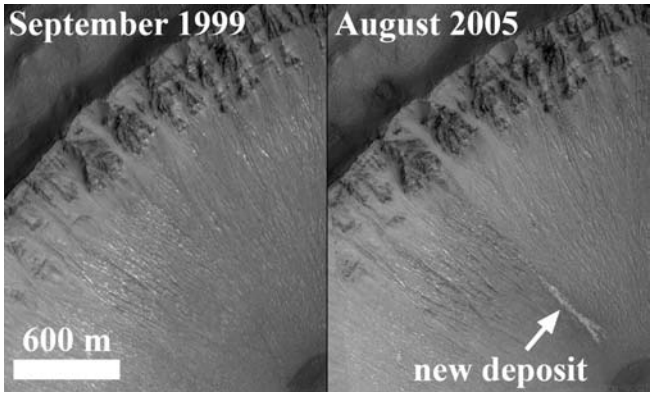

Figure 1 - Photos from the Mars Global Surveyor orbiter camera showing recent flows in a crater of the Centauri Montes region.

For exploring challenging topographies, an actively controlled tether combined with a conventional mobility platform (using e.g. wheels, legs, or tracks) may provide a useful means to enable very steep terrain access. One such example was the *Dante* tethered robot [10] that descended into the Mt. Spurr volcano in 1994 using its tether and an 8-legged walking frame. In the 1990's, following orbital imagery of Mars stratigraphy, a number of different mission concepts were proposed for *in situ* science investigations that included legged and wheeled robots. The *Cliff-bot* [11] was an example of a wheeled robot that used a dual tether system to help manage its traverse across a cliff face, which has been demonstrated on cliff faces in Svalbard, Norway. In addition to the legged and the multiple wheeled robot approaches, some of the earlier concepts also advocated the potential advantages of using lightweight tethered platforms, though none of these efforts led to an implementation.

3. THE AXEL SYSTEM: OVERVIEW

In order to provide access and in-situ sampling in areas of extreme terrain, the Jet Propulsion Laboratory (JPL) and the California Institute of Technology (Caltech) have been collaborating to develop the Axel rover. Axel is a minimalistic robot consisting of two wheels connected by a central cylindrical body, a caster arm, and an actively controlled tether passing through the caster arm (Figure 2). The caster arm, in addition to controlling the tether, also provides a reaction force against the terrain necessary to generate forward motion when travelling on flat ground.

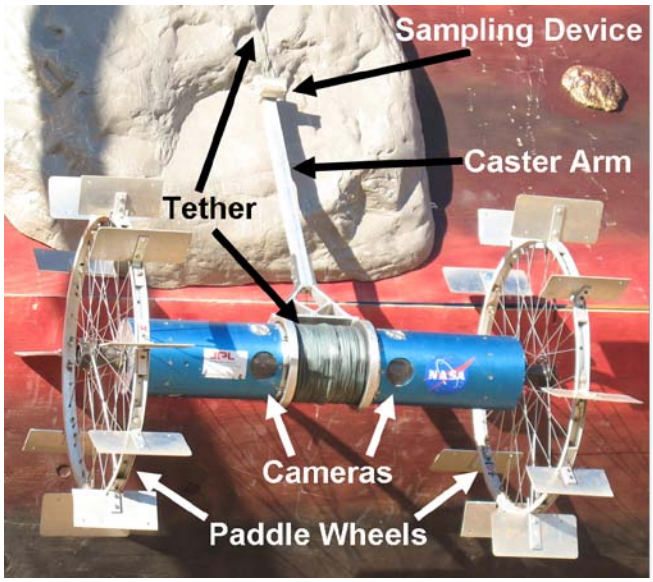

Figure 2 – Photograph of Axel with key features labeled.

Axel's minimalist design overcomes some of the limitations found in prior tethered robots. *Dante*'s operation on Mt. Spurr was cut short when it tipped over—it had no built-in mechanism to recover an upright posture. Due to its symmetry, Axel has no upside-down posture and thus does not suffer from this failure mode. Cliffbot similarly has no tip-over recovery and uses two tethers. Like Dante, Axel's tether is paid out by an on-board motor, an advantage compared to Cliffbot's more complicated off-board tether management system. Due to Axel's low mass, on-board battery, and wireless communication link, the tether is a simple high strength cord as opposed to Dante's heavy tether with embedded power and signal conductors.

Axel's minimalist design satisfies many of the severe constraints imposed by space mission design. Because the rover uses only three actuators to control its wheels, caster arm, and tether, its total mass is low (the current prototype weighs ~22 kg, and we expect a smaller flight qualified version with a mass of ~8-10 kg). Its simplistic design improves mechanical robustness. All of its electronic components can be centralized in the body, simplifying thermal control design for operation in extreme cold.

Mission Concept. We expect Axel to operate in hazardous terrain via the use of a host platform as an anchor. Since Axel's body acts as a winch, the host platform requirements are reduced to a simple mount. The host platform could be a lander, a larger rover, a habitat, or even an astronaut. Once the anchor point has been secured, Axel can descend overstep promontories, navigate through rocky terrain, take images, collect soil samples, and then return by reeling in its tether. Figure 3 portrays a hypothetical scenario in which Axel is deployed from the Mars Science Laboratory (MSL) [12], an example of a host platform that could potentially carry an Axel as a method of sampling in extreme terrain.

There are some key advantages to this tethered approach for planetary exploration missions. The risk to overall mission success of descending into craters or similar topographies is minimized, as the host can detach Axel's tether should it fail and then continue with other mission objectives. Axel is also small and light enough for more than one copy to be hosted from an MSL class rover. Because Axel can operate without a tether, depending on the nature of the failure, Axel may be able to continue its exploration to some level. Second, since Axel itself is the winch, the tether is laid over the terrain as the rover descends, and it is collected as the rover returns to the host. In contrast to a winch mounted on the host, our approach minimizes abrasion on the tether from rocks and cliff faces. Finally, the anchor and tether system allows Axel to travel over cliff promontories with slope angles greater than 90°, which would not be possible with an independent wheeled rover.

Figure 3 – Proposed mission concept overlaid on false color image of Victoria Crater. Note that the rover graphics are not to scale.

Prototype System. Axel measures 1 m from wheel edge to wheel edge and 0.75 m from the body's center to the end of the caster arm. The paddle wheels are 0.74 m in diameter.

Axel's body houses and protects all of its hardware and electronic components. Computations are performed by a 700 MHz Pentium processor with 128 MB of RAM and a 2 GB solid state drive. The wheels are each driven by a 30V Servodisc drive coupled to a harmonic drive. The entire system is controlled remotely via an 802.11b wireless link. Axel's 24V, 4.2 amp-hour battery allows for one hour of continuous driving before it must be recharged. A safety

circuit, which brakes the caster motor in case of sudden power loss, ensures a slow and controlled descent, eliminating the need for a safety tether.

Stereo cameras are located as shown in Figure 2 in order to make room for the tether. The two PointGrey 1024x768 color Firewire cameras have a 25 cm baseline. Fujinon lenses with 105º field-of-view provide reasonable visibility so that a human teleoperator could drive the rover from a remote position. In tumbling mode, primarily used to reel and unreel the tether during ascent/descent, Axel's cameras rotate with its body, producing images at different pitch angles. To control the pitch at which images are acquired, an inertial measurement unit (MicroStrain 3DM-GX1) triggers image acquisition. By acquiring consecutive images at the same pitch, a more intuitive image map can be constructed, which simplifies human teleoperation as well as autonomous map-based motion planning.

At present, we have a simple soil sampling system to allow for experimentation with sample acquisition strategies in extreme terrain. This sampling device (Figure 4 insert) features two sample containers mounted on the end of the caster arm, perpendicular to its long axis. After pushing the caster arm into the ground, Axel oscillates around its center, thereby scooping soil into the tubular containers. The tubes face opposite directions, enabling the collection of two separate samples. Furthermore, the containers are detachable so that the host platform rover could potentially remove the sample for scientific analysis. This method works well for loose soil and on slopes ranging from 0 to 40 degrees.

Figure 4 – Axel taking a sample by pointing the caster arm into the ground and turning in place. Sand enters through the openings on the ends of the removable sampling tubes (inset).

Because Axel's potential extreme terrain mobility are dependent upon the combination its tether and wheels, the following sections analyze these components.

4. WHEEL DESIGN

Descending crater walls and navigating over loose sediment and rocky terrain persists as a difficult challenge for rovers, whose performance in these scenarios depends greatly on the type of wheels they carry. Thus, we have exerted some effort on the design and optimization of Axel's wheels for our particular goal of extreme terrain exploration. As seen in Figure 2, Axel uses an unusual wheel design that combines a conventional wheel rim with evenly spaced "paddles." A simplified physics model will now be presented in order to help build a better understanding of how Axel's wheels drive over obstacles.

While obstacle traversal is greatly improved by the use of a tether, Axel must be able to operate independently while on flat ground. Therefore, in order to focus particularly on wheel optimization, the tether input is excluded from the analysis.

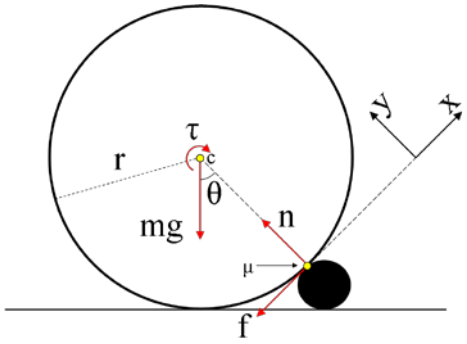

Figure 5 – Free-body diagram of a wheel travelling over a rock just as it loses contact with the ground.

Figure 5 represents the forces experienced by a wheel just as it loses contact with the ground after encountering an obstacle. While obstacle shapes in the field can be quite complicated, for simplicity we consider an object with circular cross section. The wheel contacts the obstacle at a point along its rim θ radians from the vertical. The coefficient of friction between the wheel and the obstacle is denoted by μ, while τ represents the torque applied to the wheel by the motor. Summing the forces and moments:

$$\sum F_x = ma = -f - mg\sin\theta \quad (1)$$

$$\sum F_y = 0 = n - mg\cos\theta \quad (2)$$

$$\sum M_c = I\alpha = -fr - \tau \quad (3)$$

Note that $\alpha = -a/r$ and $|f| < |\mu n|$ for the wheel to travel without slipping. After rearranging and solving, we find that for the wheel to have a positive acceleration in the x-direction (a>0, thereby continuing over the obstacle), two conditions must be met for $0 \le \theta < \pi/2$:

$$\tau > mgr\sin\theta; \qquad \mu > \tan\theta \quad (4)$$

Notice that as θ approaches $\pi/2$, the magnitude of μ must tend toward infinity if the wheel is to climb over the obstacle. Without the aid of a tether, the wheel cannot surpass obstacles whose contact point height is greater than one-half of the wheel diameter above the ground plane.

Traditional wheels are therefore fundamentally limited in terms of their performance over obstacles.

However, with a slight modification the wheel forces can be redirected in the rover's favor. Figure 6 presents a free-body diagram of a wheel with 5 equidistant "paddles" as it encounters an obstacle and just as it leaves the ground. This wheel provides a motion that is roughly a hybrid of rolling and walking. Letting l denote the length of the paddle, Newton's second law applied to Figure 6 yields:

$$\sum F_x = ma_x = 0 = -f + mg\cos\theta \tag{5}$$

$$\sum F_y = ma_y = n - mg\sin\theta \tag{6}$$

$$\sum M_c = I\alpha = -\tau + n(r+l) \tag{7}$$

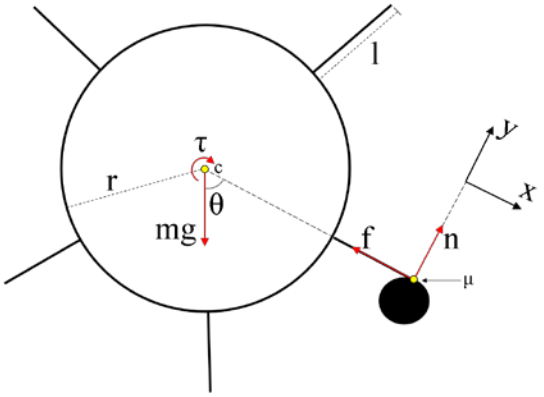

Figure 6 – Force diagram of a paddle-wheel as it encounters an obstacle and just as it leaves the ground.

For the wheel to travel over the obstacle without slipping, note that $\alpha = -a/(r+l)$ and once again $|f| < |\mu n|$. To ensure forward movement over the obstacle ($a > 0$) when $0 \le \theta < \pi/2$, two conditions must be met:

$$\tau > mg(r+l)\sin\theta \tag{8}$$

$$\mu > \frac{g\left(I + m(r+l)^2\right)\cos\theta}{Ig\sin\theta + \tau(r+l)} \tag{9}$$

Note that since the lower bound on the coefficient of friction is inversely proportional to input torque, this bound can be reduced by increasing the wheel torque. Furthermore, the lower-bound on μ approaches zero as the contact point angle, θ, approaches $\pi/2$. Thus, with a paddle-wheel design, for a small increase in the required torque, it actually becomes easier to travel over obstacles without slipping, especially as the contact point angle increases.

If the paddle-wheel can slip in the x-direction, the equations of motion become:

$$\sum F_x = ma_x = -f + mg\cos\theta \tag{10}$$

$$\sum F_y = ma_y = n - mg\sin\theta \tag{11}$$

$$\sum M_c = I\alpha = -\tau + n(r+l) \tag{12}$$

Here we simplify on the condition that $a_x > 0$ for $0 \le \theta < \pi/2$ while noting that $|f| = |\mu n|$. As expected, the input torque requirement is the same as in the no-slip case while the bound on the coefficient of friction becomes:

$$\mu < \cot\theta \tag{13}$$

Hence for small angles the paddle-wheel travels over obstacles while slipping. As the contact point angle increases, one can expect the paddle-wheel to stop slipping and switch to the previous equations of motion. Note that this is in contrast to the traditional wheel, which, at the low wheel rotation speeds characteristic of rovers, cannot overcome an obstacle while slipping.

In summary, a simplified physics model of the paddle-wheel predicts that it will perform better than a traditional wheel at higher contact point angles. At smaller angles, we expect that the paddle-wheel will generally overcome the obstacle while it slips along the paddle.

A rigorous analysis of the performance of Axel's wheels over deformable terrain is beyond the scope of this paper and will be the subject of future investigation. The research is particularly important for Axel because low-cohesion soils are characteristic of the extreme terrain environments encountered on the Moon and on Mars. Relevant work in this field can be found in the references [13, 14].

5. TETHER LOADING ANALYSIS

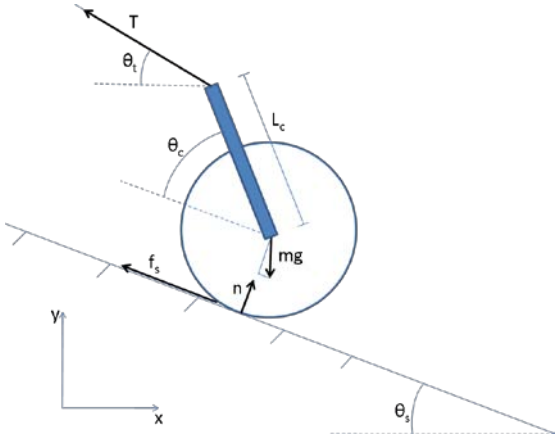

Figure 7 - Two-dimensional free-body diagram of tethered Axel on a slope.

Axel can descend over crater promontories and ascend steep slopes primarily because of its ability to manage its own tether. Tensile strength, resistance to shear, mass, and diameter are all important factors when selecting a tether. We begin with an analysis of the tensile forces experienced by the tether, which helped us to determine the minimum breaking tether strength required to support the Axel rover.

Figure 7 shows a 2-dimensional free-body diagram of a tethered Axel on a slope. In a quasi-static analysis, the equations of motion are:

$$\sum F_x = 0 = -T\cos\theta_t - f_s\cos\theta_s + n\sin\theta_s \quad (14)$$

$$\sum F_y = 0 = T\sin\theta_t + f_s\sin\theta_s + n\cos\theta_s - mg \quad (15)$$

$$\sum M = 0 = T\cos\theta_t L_c\sin(\theta_c+\theta_s) - T\sin\theta_t L_c\cos(\theta_c+\theta_s) - f_s r_w \quad (16)$$

Solving for the tether tension, we find

$$T = \frac{mgr_w\sin\theta_s}{L_c\sin(\theta_c+\theta_s-\theta_t)+r_w\cos(\theta_s-\theta_t)} \quad (17)$$

For our particular model, Axel's weight mg, wheel radius r_w, and caster length L_c are 50 lbs, .54 ft, and 2.3 ft, respectively. Hence, the tether tension is a function of the slope, tether angle, and caster angle. Figure 8 shows theoretical tension for a 30° slope angle and a range of tether and caster angles (physically unrealizable configurations were excluded). Figure 8 shows that, in the static case, the theoretical maximum tether tension on a 30 degree slope is around 50 lbs, which approximates Axel's weight.

Tether Tension Experiments. The accuracy of the tether tension analysis was verified via an experiment conducted using a 250 lb capacity tension sensor (Omega Engineering LC101). The sensor was mounted in-line with the tether near the anchor point. During the experiment, Axel was balanced statically on a sloped board. Measurements were taken for 3 different slopes and 6-9 different caster angles.

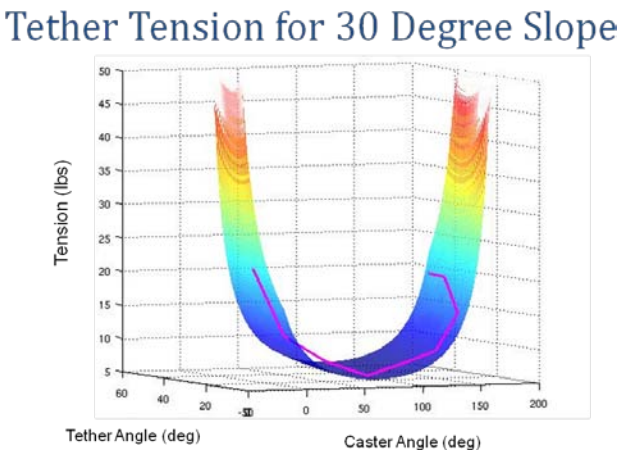

Figure 8 – Predicted tether tension vs. tether and caster angle for 30° slope. Measured tension, represented by the purple line, is overlaid on the theoretical prediction.

The data from the 30° slope experiment (overlaid on the model in Figure 8) fits the predicted values reasonably well, and never deviates from the model by more than 11 lbs.

Tether tension over precipices and crater entries. Ascending over a ledge, from a 90 degree slope to a 0 degree horizontal, poses a practical challenge for Axel—the caster motor may stall during this maneuver due to a significant increase in the required torque. Here we develop a quasi-static model to better understand this maneuver.

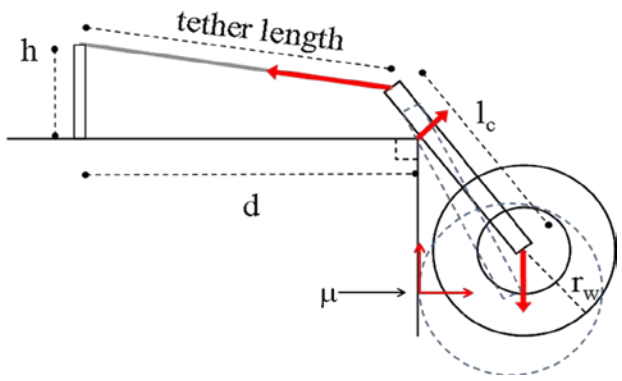

Figure 9 – Free body diagram of Axel ascending over a ledge. Initially wheels are in contact with the wall, but separate from the wall as winching progresses.

A 2-dimensional free body diagram of Axel climbing over a 90 degree ledge can be seen in Figure 9. The important parameters for this model are the wheel radius, r_w, the caster arm length, l_c, the coefficient of friction between the wheel and the wall, μ, and the anchor point's height and distance from the corner, h and d, respectively.

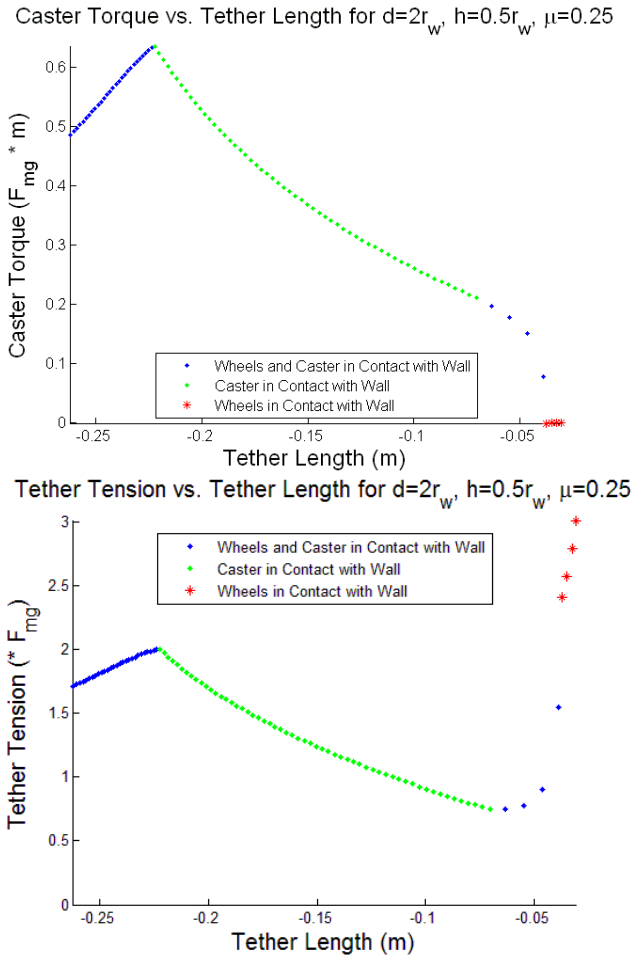

Figure 10 – Caster motor torque (top) and tether tension (bottom) vs. tether length for geometry of Figure 9.

If the ratio of wheel radius to caster length is sufficiently small, and the anchor height is low, Axel will reach a configuration where its wheels lose contact with the

wall, and the torque on the caster arm required to continue ascent is at a maximum. Figure 10 plots the estimated caster motor torque and tether tension as the rover ascends over the lip. Note that the x-axis represents the negative of the unreeled tether length, corresponding to Axel's ascent over the ledge in time from left to right. A spike in tether tension occurs when the wheels lift from the wall. The theoretical tension approaches an infinite value just as the wheels approach the corner of the ledge. With a low anchor point, the rover must pull very hard on the tether to generate any upward force since the tension vector is nearly horizontal.

This potentially hazardous scenario can be simply avoided by increasing the height of the anchor point. By doing so, the wheels will remain in contact with the wall and can help drive the rover over the ledge. From Figure 11, one can see that by increasing h, the tether tension can be minimized and kept below the rupture stress.

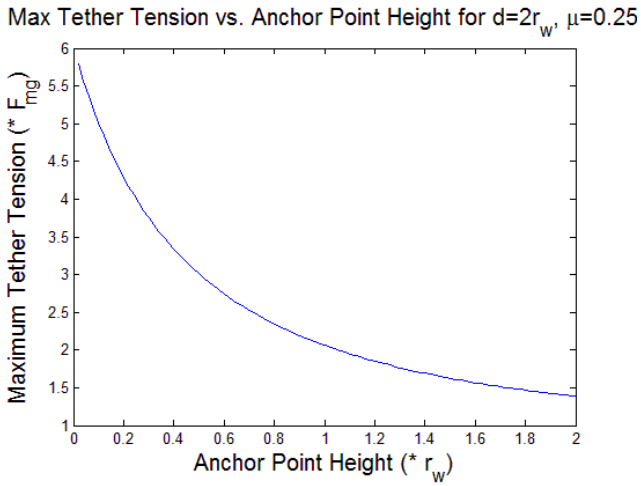

Figure 11 –Tether tension vs. tether length for geometry of Figure 9, with higher anchor point.

Based on these calculations, and a safety factor of 2.5 for dynamic loading, we were able to select a very lightweight composite fiber tether with a 1 kg mass for its 1km length. This length is sufficient to access many of the scientifically interesting features reviewed in Section 1.

6. Tether Management

Fully automated operation requires a methodology to plan Axel's ascents and descents in complex terrain. Although Axel is relatively simple, the problem of motion planning and obstacle avoidance for tethered robots on steep terrains has not been well considered. Prior work has considered motion planning for planar robots with trailing tethers so as to prevent tether entanglement [15,16], or free flying robots anchored by tethers [17]. However, in these prior works, the tether tension was not critical to the mobility of the robotic vehicle. The general problem of active tether management and control on complex steep terrain is a large subject which we only briefly touch upon.

A primary problem is to determine Axel's path during descent so that when it returns to the host, Axel does not become "snagged," or "wedged"—conditions where Axel cannot reel in its tether, thereby preventing ascent. Here we sketch conditions under which Axel cannot free itself when the tether hugs an obstacle. Knowledge of the key factors influencing such situations can help us plan to avoid them during Axel's descent and ascent.

Several assumptions simplify the analysis. First, we assume that Axel operates on a slope of angle θ_s which is populated by cylindrical obstacles (Figure 12). Our analysis holds for more general object shapes, with the local radius of object curvature modeled by the cylinders. Axel's movements are restricted to the slope, except for the caster arm moving in the plane normal to the slope. Let Axel lie at a posture as in Figure 12 with the tether partially wrapped around the closest obstacle as Axel ascends.

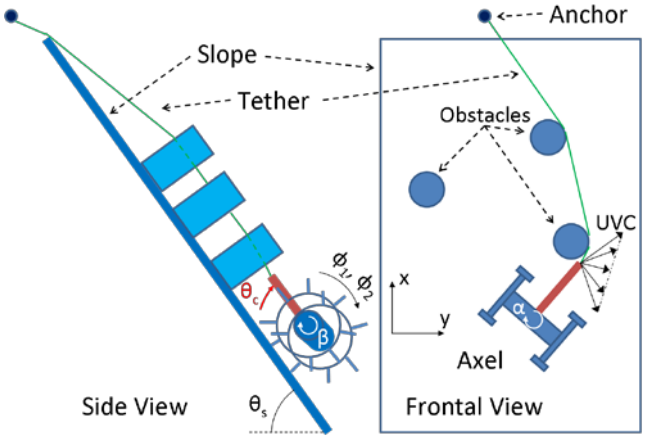

Figure 12 –Schematic Diagram (side and frontal views) of Axel on slope with obstacles.

While reeling in its tether, Axel may become stuck against an obstacle, preventing further winding of the tether. Axel can get "unstuck" if it can locally maneuver so as to unwrap the tether from the obstacle. A complete analysis of such maneuvers is the subject of ongoing work. However, it is sufficient if Axel's motors can generate a local motion in the *unsnagging velocity cone* (UVC, Figure 12). Axel velocities inside this cone will move the tip of the caster arm so as to unwrap a small amount of tether from the obstacle.

Checking the feasibility of such motions requires a dynamic model. Using a Lagrangian approach, we first define q as the vector of Axel configuration variables:

$$q = (x, y, \alpha, \beta, \phi_1, \phi_2, \theta_c).$$

Here, x and y refer to the position of Axel's body in the plane of the slope, and α is the body angle with respect to the up-slope direction. The variables β, φ_1, and φ_2 denote the body and wheel angles around the body-fixed y-axis, respectively, and θ_c is the caster arm angle.

To obtain the correct equations of motion, we must apply constraints as demanded by a particular scenario. The tether constrains the system such that the distance between Axel and the point of entanglement can be no greater than the length of unreeled tether, l_t (assuming that the caster motor is not rotating, and that tether elongation under load is negligible). The movement of the caster arm is restricted

such that it cannot penetrate the ground. Under these assumptions, the tether and caster arm ground reaction forces can be modeled as a set of two independent holonomic inequality constraints of the form $h_j(q) \le 0$, $j = 1,2$.

A model for the wheel-ground interaction forces can be quite complex, and dependent upon the soil type [13, 14]. For purposes of discussion, assume that a Coulomb friction model governs Axel's ground contact. Assuming Axel rolls upon the ground without slipping, its motion is governed by nonholonomic constraints of the form $\omega(q)\dot{q} = 0$. Including these constraints, the Euler-Lagrange equations take the form

$$M(q)\ddot{q} + B(q,\dot{q}) + G(q) = C^T(q)\Lambda + \tau \qquad (18)$$

where τ is the vector of wheel and caster motor torques, *M(q)* is a definite symmetric mass matrix, *B* is the vector of Coriolis forces, *G(q)* denote gravitational forces, *C(q)* arises from the constraints, and Λ are the undetermined Lagrange multipliers that correspond to the tether, caster, and wheel reaction forces (assuming the constraints are active) [18]. Solving for the Lagrange multipliers, substituting the fully determined multipliers into Equation (18), and assuming that Axel is at rest (so that *B*=0), we get:

$$\begin{aligned} \ddot{q} &= (M^{-1} - M^{-1}C[C^T M^{-1} C]^{-1} C^T M^{-1})[\tau - G] \\ &\equiv K[\tau - G] \end{aligned} \qquad (19)$$

Starting from rest, Axel's motions can be approximated by $\dot{q} \approx \ddot{q}\Delta t$ for small time Δt. Thus, axel can successfully maneuver if there exists at configuration *q* a feasible set of motor torques τ such that:

$$K(q)[\tau - G(q)] \in UVC(q) \qquad (20)$$

where *UVC(q)* is the unsnagging velocity cone at configuration *q*.

In practice, one or more of Axel's wheels may slip as it maneuvers around the obstacle, and the tether and caster constraints may become intermittently active and inactive. It is not possible to model these issues with enough precision to predict when Axel will switch between different models that govern its behavior. Thus, Axel's dynamics represent a *multiple model control system* [19], and Axel's ability to locally maneuver around an obstacle can be formally posed as a problem in *multiple model controllability* [19], which is beyond the scope of this paper.

7. Mobility Experiments

Experiments to test Axel's capabilities were conducted in the *Mars Yard* at the Jet Propulsion Laboratory. To simulate the exploration of a Martian crater, we created a promontory with a 90° slope and secured a mock lander near the top of the "crater" to serve as the anchor and starting point for Axel's trials. Using teleoperation, we demonstrated Axel's ability to descend down slopes 90 ° or greater, traverse to flat ground, sample loose soil on slopes ranging form 0 ° to 40 °, travel over rocky terrain, and finally ascend back up the vertical promontory to its original starting position (Figure 13).

Figure 13 – Left column from top to bottom: Axel descending down onto sloped terrain in the JPL Mars Yard. Right column from bottom to top: Axel ascending over a simulated crater promontory onto a mock lander.

Figure 14 – From top-left to bottom right: Axel uses its large radius paddle wheels to traverse over a rock more than half of its wheel diameter in the JPL Mars Yard.

We conducted 15 runs, each round trip taking about 20 minutes and extending 30 m from the anchor point. A summary video can be found at

http://robotics.caltech.edu/~pablo/axel/movies_2009.01

The paddle wheels were effective at climbing over rocks at least ½ of the wheel diameter, both independently and with the aid of the tether (Figure 14). As the simulation of Section 5 predicted, the large wheel radii facilitated the return ascent over the promontory. Furthermore, the tether never ruptured from overstress.

8. Conclusions and Future Work

We presented a minimalist tethered robotic rover, Axel, whose low mass, simplicity, and robustness make it a viable candidate for future explorations of extreme planetary terrains. While we envision that Axel will be deployed via a tether from a host rover or lander, its simplicity and low mass would allow it to be used in various mission designs.

This paper focused on issues of wheel design, tether stress, and tether management, which are essential components for successful deployment of Axel in extreme terrain. We have shown that a modified wheel design provides Axel with a greater capability to traverse rocky terrain and climb moderate slopes without a tether. We have also demonstrated the effectiveness of the paddle-wheel design in travelling over obstacles greater than one-half wheel diameter. We also summarized experimental work showing Axel's ability to negotiate simulated extreme terrains of the type that might be encountered in future missions. Ongoing and future work seeks to develop a more sophisticated computational model involving the complex wheel-soil interaction. Such improved models would then lead to advanced planning algorithms that would allow Axel to complete its goals autonomously.

Acknowledgments. The work of this collaboration between Caltech and the Jet Propulsion Laboratory was performed at JPL under contract to the National Aeronautics and Space Administration. The authors sincerely appreciate the sponsorship of the Exploration Systems Mission Directorate and Solar Systems Exploration program: Dr. C. Moore, Dr. S. Khanna, Dr. T.Y. Yan, Dr. J. Cutts, and Dr. K. Reh. We also appreciate the support of Dr. S. Hayati, Dr. R. Volpe and Dr. G. Udomkesmalee of JPL.

References

[1] http://marsrovers.jpl.nasa.gov/home/index.html

[2] E. Kraal, M. Dijk, G. Postma, M.G. Kleinhans, "Martian stepped-delta formation by rapid water release," *Nature* **451**, Feb. 21, 2008, pp. 973-976.

[3]http://www.nasa.gov/mission_pages/mars/news/marsmethane.html

[4] K.J. Waldron, Machines that Walk: the Adaptive Suspension Vehicle, MIT Press, Cambridge, Mass., 1989.

[5] M. Hirose and K. Ogawa, "Honda humanoid robots development," *Phil. Trans. Royal Soc. A*, **365**(1850):11-19, Jan. 2007.

[6] J. Burdick an P. Fiorini, "Minimalist Jumping Robots for Celestial Exploration," *Int. J. Robotics Research, vol. 22, no. 7-8, pp. 653-674, Aug. 2003.*

[7] G.S. Chirikjian and J.W. Burdick, "The Kinematics of Hyper-Redundant Locomotion," *IEEE Trans. Robotics and Automation*, vol. 11, no.6, pp. 781-793, Dec. 1995.

[8] M. Lamboley, C. Proy, L. Rastel, T.N. Trong, A. Zashchiriski, and S. Buslaiev, "Marsokhod Autonomous navigation tests on a Mars-like Terrain," *Autonomous Robots*, **2**(4):1573-7527, Dec. 1995.

[9] D. Miller, T.L. Lee, "High-Speed Traversal of Rough Terrain Using a Rocker-Bogie Mobility System," *Roving over Mars, Mechanical Engineering*, April 1998, pp. 74-77.

[10] J. Bares and D. Wettergreen, "Dante II: Technical Description, Results and Lessons Learned," *Int. J. Robotics Research*, Vol. 18, No. 7, July, 1999, pp. 621-649.

[11] E. Mumm, S. Farritor, P. Pirjanian, C. Leger, P. Schenker, "Planetary cliff descent using cooperative robots," *Autonomous Robots*, Vol. 16, No. 3, May, 2004, pp. 259-272.

[12] http://mars.jpl.nasa.gov/msl/

[13] H. Shibly, K. Iagnemma, S. Dubowsky, "An Equivalent Soil Mechanics Formulation for Rigid Wheels in Deformable Terrain, with Application to Planetary Exploration Rovers," *J. Terramechanics*, vol. 42, no. 1, pp. 1-13, Jan. 2005.

[14] G. Scott, G. Meirion-Griffith, C. Saaj, El Moxey, "A Comparative Study of the Deformation of Planetary Soils under Tracked and Legged Rovers," *Proc. AIAA Space Conference & Exposition*, September 2008.

[15] F.W. Sinden, "The Tethered Robot Problem," *Int. J. Robotics Research, vol. 9, no. 1, pp. 122-133*, Feb. 1990.

[16] P.G. Xavier, "Shortest Path Planning for a Tethered Robot or an Anchored Cable," *Proc. IEEE Int. Conf. Robotics and Automation*, pp. 1011-1017, Detroit, MI, May 1999.

[17] P. McKerrow and D. Ratner, "The Design of a Tethered Aerial Robot," *Proc. IEEE Int. Conf. Robotics and and Automation*, pp. 1011-1017, Detroit, MI, May 1999.

[18] R. Murray, Z. Li, S. S. Sastry, A Mathematical Introduction to Robotic Manipulation, CRC Press, Boca Reton, Fla., 1994.

[19] T. Murphey and J.W. Burdick, "A Local Controllability Test for Nonlinear Multiple Model Systems," *Proc. 41st Conf. on Decision and Control*, Dec. 2002.